EurJOC European Journal of Organic Chemistry

FULL PAPER

DOI: 10.1002/ejoc.201200879

Turning On Fluorescence with Thiols – Synthetic and Computational Studies on Diaminoterephthalates and Monitoring the Switch of the Ca^{2+} Sensor Recoverin

Nina Wache,[a] Alexander Scholten,[b] Thorsten Klüner,[a] Karl-Wilhelm Koch,[b] and Jens Christoffers*[a]

Keywords: Fluorescent probes / Sensors / Calcium

The fluorescence of maleimide-functionalized diaminoterephthalate derivatives (NiWa Orange) is "turned on" by the conjugate addition of thiols. Three new representatives of this class of dyes with emission at 560 nm were synthesized from succinyl succinates. The mechanism of turning on the fluorescence was investigated by computational studies. Radiationless transition to an energetically low-lying excited state by a nonadiabatic interaction was the mechanism leading to absence of fluorescence prior to the reaction of the probe with its molecular target. This concept was proven by labeling cysteine-containing peptides and proteins. For example, the single cysteine residue at position 39 of the neuronal calcium sensor protein recoverin binds to NiWa Orange and turns on its fluorescence. The Ca^{2+}-dependent Förster resonance energy transfer (FRET) process from a tryptophan residue in proximity to Cys39-bound NiWa Orange was used for the determination of differences in Ca^{2+}-binding affinities of myristoylated and nonmyristoylated recoverin.

Introduction

The fluorescent labeling of proteins is a powerful and reliable tool in biochemistry, medicine, and biology, allowing for the fast and precise investigation of the dynamics, interactions, and localizations of proteins.[1] Several labeling techniques use fluorescent dyes with a reactive functional group such as the maleimide moiety, which is well known to react with protein surfaces holding thiol functions.[2] A prominent example of such a dye is the fluorescein derivative **1** (Scheme 1).[3] There is a class of compounds that are not luminescent themselves, but their fluorescence is "turned on" upon the conjugate addition of a thiol to the maleimide function of the dye.[4] The boron dipyrromethene (BODIPY) derivative **2** is an example of such a so-called turn-on probe.[5]

The preparation of diaminoterephthalates, which have been known for almost 100 years,[6] starts from succinyl succinates[7] and primary amines and is therefore relatively simple. However, these dyes are hardly found in the literature,[8] although they are brilliant dyes with pronounced fluorescence behavior. In continuation of our work on diaminoterephthalates as fluorescent dyes,[9] we have recently reported on the preparation of the thiol-reactive turn-on fluorescent probe **3** (NiWa Blue). Upon reaction with BnSH, the product **4** showed fluorescence at 391 nm when excited at 338 nm (Scheme 1).[10] Its utility as a tool in biochemistry was proven by staining of the neuronal calcium sensor re-

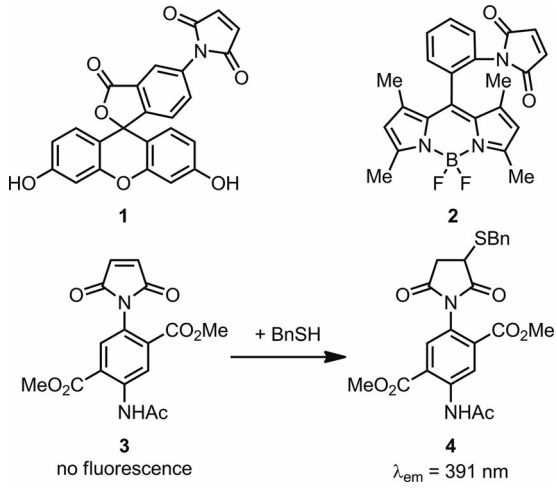

Scheme 1. Thiol-reactive fluorescence probes with a maleimide moiety. Whereas fluorescein derivative **1** shows luminescence even without addition of a thiol, **2** and **3** are nonemissive; their fluorescence is turned on by the conjugate addition of a thiol, as is shown for the formation of **4** from dye **3** (NiWa Blue).

[a] Institut für Chemie, Carl von Ossietzky Universität, 26111 Oldenburg, Germany
Fax: +49-441-798-3873
E-mail: jens.christoffers@uni-oldenburg.de
Homepage: www.christoffers.chemie.uni-oldenburg.de
[b] Institut für Biologie und Umweltwissenschaften, Carl von Ossietzky Universität, 26111 Oldenburg, Germany
Supporting information for this article is available on the WWW under http://dx.doi.org/10.1002/ejoc.201200879.

coverin, which plays a major role in the photoreceptor function in vertebrate retina.[11] Recoverin possesses four EF-hand motifs as Ca^{2+} binding sites, of which only the second and third are functional. One Cys residue lies in position 39 on the surface of this protein and is therefore susceptible to reactions with maleimide.[12] The Ca^{2+}-free and the Ca^{2+}-bound state of recoverin adopt two significantly different conformations that can be tracked by biochemical and biophysical methods. For example, the thiol-sensitive fluorescent dye **3** was recently employed to monitor Ca^{2+}-induced conformational changes in recoverin.[10] This dye is turned on by covalent attachment to recoverin and shows fluorescence emission at about 440 nm irrespective of the presence of Ca^{2+}. However, Ca^{2+}-induced conformational changes in recoverin lead to intensity changes in Trp fluorescence emission, which by a Förster resonance energy transfer (FRET) process can excite the bound NiWa Blue dye. In the absence of Ca^{2+}, a Trp residue is in proximity to Cys39 and its conjugated NiWa Blue. Upon excitation of the Trp chromophore at 280 nm FRET occurs resulting in fluorescence emission of NiWa Blue at ca. 440 nm. In the presence of Ca^{2+}, recoverin has a protein conformation with a larger distance between the Trp and Cys residues. The FRET process is therefore significantly weakened and a Trp emission at 340 nm becomes more pronounced.[10] The emission of compound **4** is in the blue region of the visible spectrum (λ_{ex} = 338 nm, λ_{em} = 391 nm in CH_2Cl_2, λ_{em} = 440 nm on the surface of the protein and in buffered solution) with a matrix-dependent Stokes shift of up to 100 nm. In order to avoid excitation of the NiWa dye (λ_{ex} = 338 nm) when irradiating into proximal wavelengths (e.g. at 280 nm for Trp excitation or other aromatic biomolecules, like cofactors, e.g. NADH),[1a] we were aiming for a more redshifted dye and wish to report herein on our results of the development of a NiWa Orange turn-on fluorescence probe for thiols.

There are two key issues combined in our diaminoterephthalate system, which are not fulfilled by so far known dyes: (1) the turn on of fluorescence by reaction with a thiol and (2) the chromophore itself defines a molecular scaffold with four points of diversification ready for further functionalization. Besides the labeling of recoverin, which we report herein, we are therefore aiming to use NiWa dyes for other applications in the future, e.g. for probing the switch of another Ca^{2+} sensor, GCAP2.[13]

Results and Discussion

Organic Synthesis

In order to generate redshifted fluorescence wavelengths by electronic decoupling of the donor and acceptor, we decided to introduce an ethylene spacer between the diaminoterephthalate and maleimide part of the compound. For this reason, diketone **5**[14] was converted with *N*-Boc-ethylenediamine[15] by a two-step procedure (Scheme 2). First of all, the double enamine was formed, with removal of water from the reaction mixture. Secondly, oxidation was achieved with careful exclusion of moisture by using synthetic air and a solution of HCl in 2-propanol as an additive. Product **6** (Scheme 2) was obtained (71% yield) as a red crystalline solid (λ_{abs} = 469 nm, λ_{em} = 569 nm, Φ = 0.26). The quantum yield was estimated by comparison with fluorescein as a standard.[16] Both carbamate protective groups were removed with trifluoroacetic acid (TFA), either neat or diluted with CH_2Cl_2, and the material was subsequently converted with maleic anhydride at elevated temperature in AcOH as solvent. In contrast to our earlier results with the preparation of **3**, we were not able to prevent double imide formation. Moreover, the mono- and bisimides could not be separated, not even after capping of the remaining amino group as an acetamide group. Therefore, we used an excess of maleic anhydride to obtain the bisimide **7** in 32% yield on a quarter-gram-scale if neat TFA was used for the deprotection. If TFA was diluted with CH_2Cl_2, the monoacetoxylated compound **8** (9% yield) was formed as a byproduct. Both products **7** and **8** could be separated by repeated chromatographies, therefore, the yields (15% of **7** and 9% of **8**) were low. In contrast to their starting material **6**, compounds **7** (λ_{abs} = 462 nm) and **8** (λ_{abs} = 446 nm) showed no fluorescence. The emission of the fluorophores seemed to be quenched by the maleimide moieties.

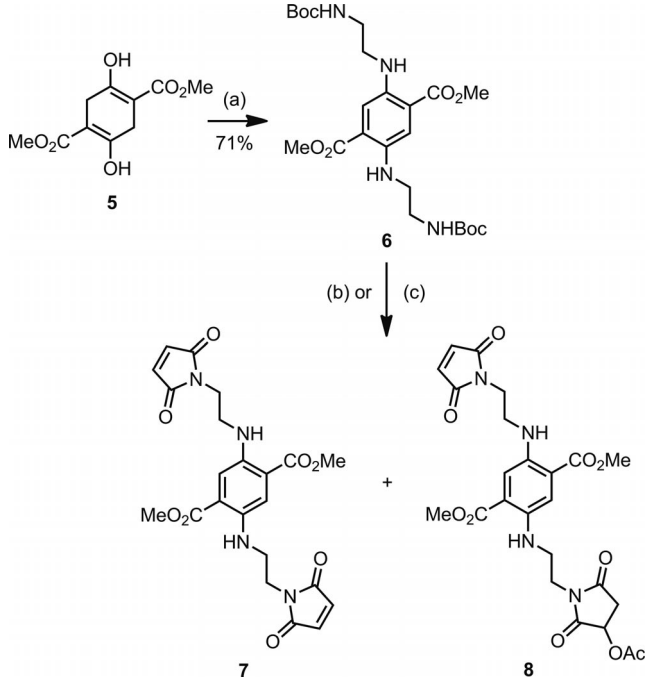

Scheme 2. Preparation of NiWa Orange I **7** and NiWa Orange II **8**. Reagents and conditions: (a) 1. 4 equiv. $BocHNCH_2CH_2NH_2$, cat. AcOH, toluene, Dean–Stark trap, 110 °C, 16 h; 2. O_2 (synthetic air), cat. HCl, *i*PrOH, *N*,*N*-dimethylformamide (DMF), 50 °C, 5 h; (b) 1. TFA, 23 °C, 0.5 h; 2. 4.0 equiv. maleic anhydride, AcOH, 95 °C, 3 d; 32% of product **7**, no compound **8** obtained; (c) 1. TFA, CH_2Cl_2, 23 °C, 1 h; 2. 4.0 equiv. maleic anhydride, AcOH, 90 °C, 2 d; 15% of product **7**, 9% of product **8**.

In order to test its utility as a turn-on probe for thiols, NiWa Orange II **8** was converted with the cysteine-containing peptide glutathione (*G*SH) on an analytical scale in dimethyl sulfoxide (DMSO, Scheme 3). Whereas **8** itself showed no fluorescence, an orange emission (λ_{em} = 568 nm) appears after a couple of minutes, when exciting at λ_{ex} = 469 nm. The experiment was performed on an analytical scale, therefore, product **9** was not isolated, but its $[M + H]^+$ signal could be clearly detected by ESI-HRMS.

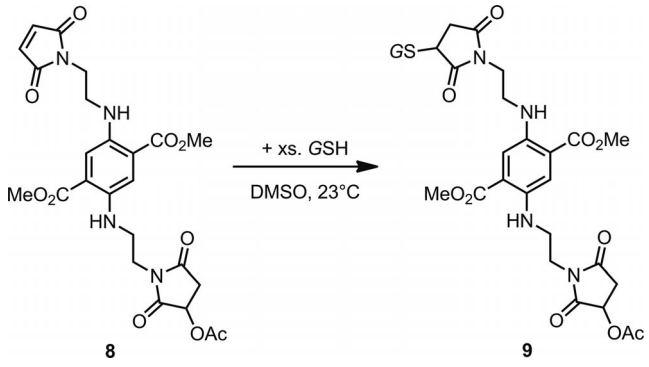

Scheme 3. Turn on of NiWa Orange II **8** with glutathione (*G*SH). Experiment on an analytical scale.

When treating NiWa Orange I **7** with an excess of BnSH, an orange fluorescence is turned on (Scheme 4). The double addition product **10** was formed and isolated on a preparative scale and spectroscopically fully characterized (λ_{ex} = 467 nm, λ_{em} = 559 nm, Φ = 0.80; Table 1). In order to obtain a compound that is turned on by only one equivalent of thiol, we aimed to prepare the mono addition product with BnSH, however, we failed, because the mono- and bis-addition products were not separable. Therefore, we applied hydrophobic *n*-hexadecanethiol for formation of the mono-addition product **11**, and indeed, it was now separable by column chromatography from remaining starting material **7** and bis-addition product **12**. In a typical experiment with 0.5 equiv. *n*-$C_{16}H_{33}SH$, products **11** and **12** were isolated in 11% and 8% yield, respectively, and compound **7** was reisolated in 19% yield. Double addition product **12** again showed strong fluorescence (λ_{ex} = 467 nm, λ_{em} = 561 nm, Φ = 0.77). The monothiol addition product **11** showed no fluorescence, as one maleimide moiety remained untouched. It is therefore an ideal probe for detecting substoichiometric quantities of thiols and was named NiWa Orange III. The fluorescence of **11** can be turned on with glutathione (*G*SH) and was again investigated on an analytical scale in DMSO. As observed for NiWa Orange II, an orange emission (λ_{em} = 565 nm) appears after a couple of minutes, when exiting at λ_{ex} = 469 nm. Product **13** was not isolated, but it was detectable by ESI-HRMS ($[M + H]^+$ signal). Compounds **10**–**12** were obtained on a preparative scale and fully characterized. Although possessing two stereocenters and therefore existing as two diastereoisomers, both **10** and **12** show only single signal sets of resonances in their NMR spectra.

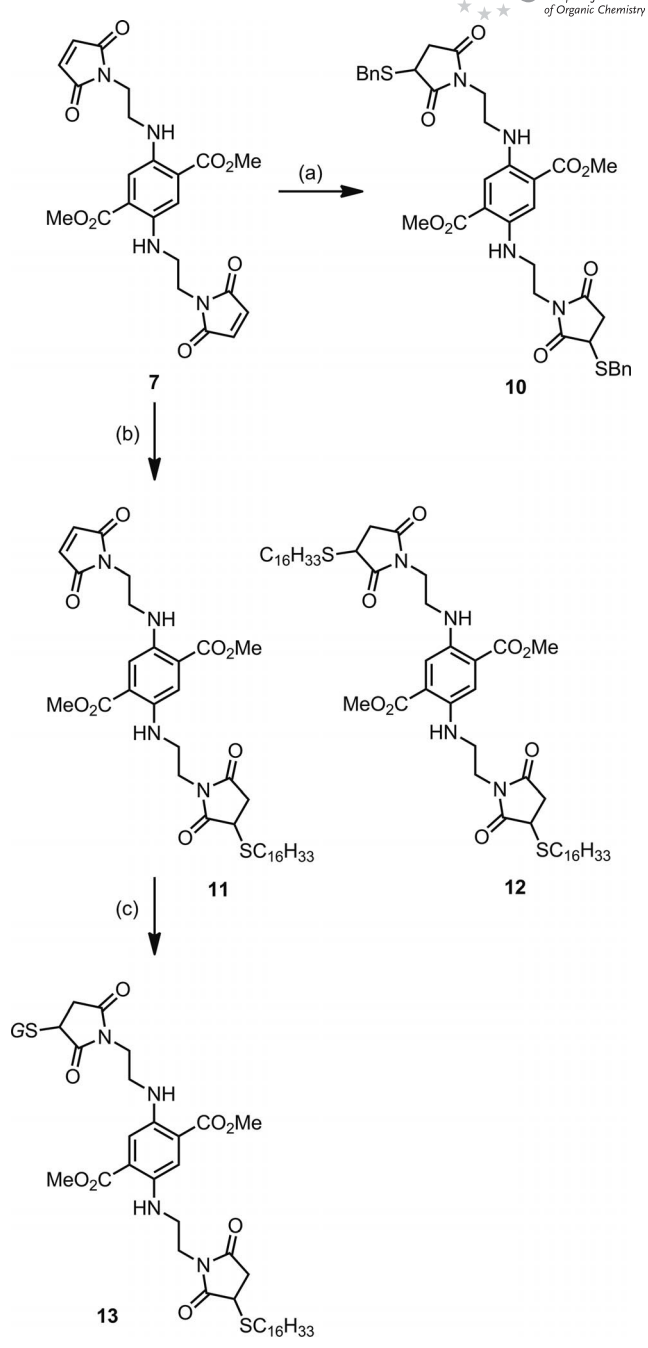

Scheme 4. Derivatization and turn on of NiWa Orange I **7**. Reagents and conditions: (a) Excess BnSH, NEt_3, CH_2Cl_2, 23 °C, 1 d, 87%; (b) 0.5 equiv. *n*$C_{16}H_{33}SH$, 4 equiv. NEt_3, CH_2Cl_2, 23 °C, 1 d; 19% starting material **7**, 11% mono adduct **11** (NiWa Orange III), 8% bis adduct **12**; (c) Excess GSH, DMSO, 23 °C, 20 min (analytical scale).

Computational Chemistry

In order to shed light on the mechanistic details of the fluorescence properties of NiWa Blue and NiWa Orange, in particular on the process of fluorescence quenching of compounds with a maleimide moiety, we performed a theoretical analysis based on time-dependent density functional theory (TDDFT) using the program package Gaussian09.[17] Throughout the study the B3LYP func-

Table 1. Spectroscopic properties of compounds **6**–**13**.

Compound	Solvent	c [10^{-4} mol dm^{-3}]	λ_{max} [nm]	ε [dm^3 mol^{-1} cm^{-1}]	λ_{em} [nm]	λ_{ex} [nm]	Φ
6	CH_2Cl_2	2.73	469	5600	569	469	0.26
7	CH_2Cl_2	2.34	462	290	–	–	–
	aqueous buffer[a]	42	445	1800	–	–	–
8	CH_2Cl_2	3.20	446	6700	–	–	–
9	DMSO	2.45	469	6700	568	469	[b]
10	CH_2Cl_2	2.23	467	3400	559	467	0.80
11	CH_2Cl_2	1.65	468	2500	–	–	–
12	CH_2Cl_2	1.52	467	4200	561	467	0.77
13	DMSO	1.25	471	2100	565	469	[b]

[a] Water/DMSO, 50:1, phosphate-buffered saline (PBS; 130 nM NaCl, 70 mM Na_2HPO_4, 30 mM NaH_2PO_4; pH = 7.4–7.5). [b] Experiments were performed on an analytical scale, no quantum yield was determined.

tional for exchange and correlation was chosen, and a 6-31+G* basis set turned out to be appropriate for sufficiently accurate calculations. Firstly, a full geometry optimization of all compounds was performed in the electronic ground state. Using the optimized geometries, we calculated vertical excitation energies and oscillator strengths for the three lowest excited states by TDDFT. The geometry of the excited state with the largest oscillator strength was optimized subsequently, and the vertical transition energy to the ground state using the excited state optimized geometry was calculated in order to obtain the fluorescence wavelength.

Firstly, we investigated the properties of **14**,[10] which experimentally showed an orange-red fluorescence (λ_{ex} = 434 nm, λ_{em} = 535 nm) as a benchmark test for our computations. Within the computational strategy outlined above, the lowest excited state shows a strong highest occupied molecular orbital (HOMO) → lowest unoccupied molecular orbital (LUMO) transition with an oscillator strength of f = 0.1034. The calculated absorption and emission wavelengths (λ_{ex} = 454 nm, λ_{em} = 544 nm, see Table 2 for all calculated data) were in very good agreement with the experimental values; this demonstrates the reliability of our computational approach (TD-B3LYP/6-31+G*) (Figure 1).

Table 2. Calculated excitation wavelength, emission wavelength, and oscillator strengths.

	Transition	λ_{ex} [nm]	λ_{em} [nm]	f
14	HOMO → LUMO (π→π*)	454 (434)[a]	544 (535)[a]	0.1034
15	HOMO → LUMO	426	–	0.0008
	HOMO → LUMO+1 (π→π*)	360	–	0.0896
16	HOMO → LUMO (π→π*)	357	400	0.0889
17	HOMO → LUMO	807	–	0.0001
	HOMO → LUMO+1 (π→π*)	470	–	0.1207
18	HOMO → LUMO (π→π*)	472	558	0.1245

[a] Experimental value in brackets.

In order to understand the absence of fluorescence of dye **3** (NiWa Blue) and the blue fluorescence of **4** after conjugate addition of a thiol, we performed corresponding calculations using **15** and **16** as simplified models.

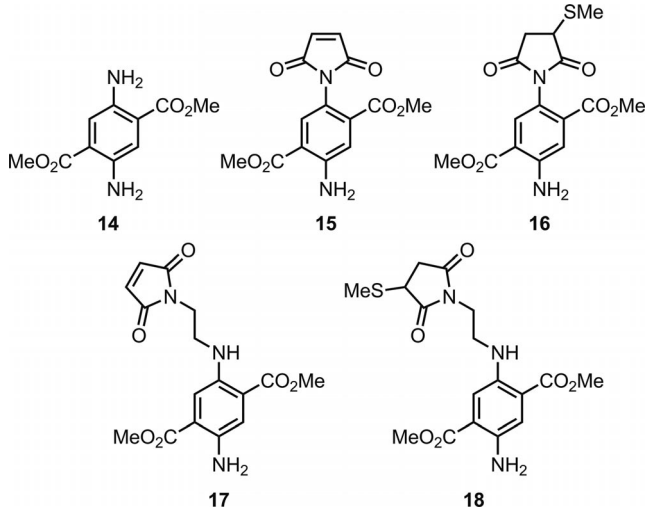

Figure 1. Compounds subjected to theoretical calculations. Dye **14** is the benchmark test system for the computational methods. Compounds **15** and **16** are structurally simplified models for **3** and its thiol addition product **4**. Compounds **17** and **18** are structurally simplified models for the NiWa Orange dyes **7**, **8**, and **11** and their thiol addition products.

Our calculations clearly indicate that **15** and **16** exhibit very similar excitation spectra. Compound **15** shows a strong excitation (λ_{ex} = 360 nm, f = 0.0896) very similar to that of **16** (λ_{ex} = 357 nm, f = 0.0889) and close to the experimental values of **3** and **4** (both with λ_{ex} = 333 nm).

However, regardless of this striking similarity of the absorption spectra, a crucial difference between the excited states manifolds of **15** and **16** was observed. In **16** the lowest excited state shows the largest oscillator strength, whereas in **15** a dark state exists, which is lower in energy as compared to the transition reported in the last paragraph but exhibits a very low oscillator strength (λ_{ex} = 426 nm, f = 0.0008). Therefore, we expect a similar excitation spectrum for both **15** and **16**, but the fate of the optically excited species will be entirely different.

After Franck–Condon excitation, **16** will geometrically rearrange because the nuclear wavefunction is not an eigenstate of the electronically excited potential energy surface (PES). Following the gradients of the excited state PES, the global minimum of the excited state might be reached eventually, which results in the expected fluorescence at this

geometry. Our calculations predict a rather strong emission with a wavelength of λ_{em} = 400 nm and an oscillator strength of f = 0.0769 in excellent agreement with experimental data for compound **4** (λ_{em} = 391 nm).

On the other hand, in compound **15** the energetically low-lying dark excited state will open an alternative route for the relaxation of the electronic excitation, which is much faster than the fluorescence of species **16** and therefore more efficient. Due to nonadiabatic coupling through a conical intersection, the system will undergo a radiationless transition to the dark state, from which an electronic relaxation is optically forbidden. Therefore, no fluorescence should be observed for NiWa Blue compound **15**, which is in perfect agreement with experimental observations.

In order to understand the differences in the excitation spectra of **15** and **16** on an atomistic level, we investigated the nature of the excited states involved in a one-particle (orbital) picture. Nevertheless, a complete mechanistic understanding would also require us to locate and to characterize the conical intersection responsible for the radiationless decay of **15** after optical excitation. However, this kind of theoretical investigation was beyond the scope of the present study, which predominantly focuses on a basic mechanistic understanding of the experimental results.

Along these lines, we investigated the nature of the lowest excited states for **15** and **16** to illustrate their different fluorescence behavior. In **16**, the lowest electronically excited state can be characterized as an optically allowed π→π* transition from the HOMO to the LUMO predominantly localized at the diaminoterephthalate moiety. Optical excitation as well as fluorescence involves a transition between these orbitals within the limits of a one-particle approximation. The corresponding molecular orbitals are displayed in Figure 2.

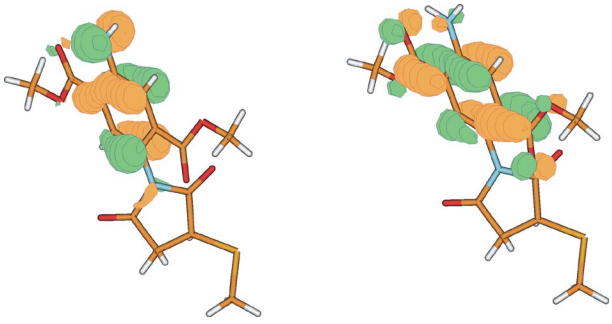

Figure 2. HOMO (left) and LUMO (right) of compound **16**. The lowest excited state corresponds to an optically allowed π→π* transition from the HOMO to the LUMO.

Similar to **16**, the NiWa Blue compound **15** exhibits an optically allowed π→π* transition from the HOMO to the LUMO+1 as the second electronically excited state of the system. However, the first electronically excited, dark state responsible for a radiationless decay in **15** can be characterized as a HOMO to LUMO transition to a charge-transfer state, in which an electron is promoted from the diaminoterephthalate moiety to the maleimide unit. The corresponding orbitals are displayed in Figure 3.

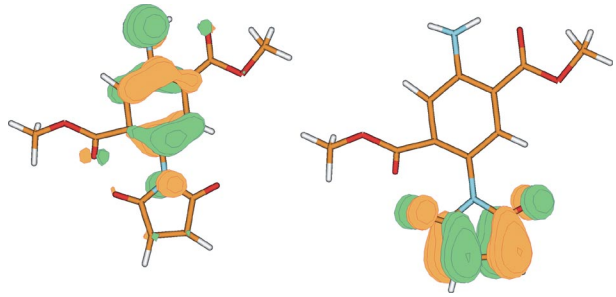

Figure 3. HOMO (left) and LUMO (right) of compound **15**. The lowest excited state corresponds to an optically forbidden charge-transfer transition from the HOMO to the LUMO.

As illustrated in Figure 3, the energetically low-lying charge-transfer excitation of **15** is not accessible by optical excitation due to a negligible HOMO–LUMO Franck–Condon orbital overlap, which results in a very small oscillator strength (f = 0.0008). However, this state plays the crucial role in quenching the fluorescence of **15** by nonadiabatic relaxation.

A similar conclusion can be drawn concerning the fluorescence properties of **17** and **18** as simplified models for the NiWa Orange dyes **7**, **8**, **11**, and their thiol addition products. Again, the absorption spectra of **17** and **18** turn out to be very similar. Compound **17** shows a strong excitation (λ_{ex} = 470 nm, f = 0.1207) very similar to that of **18** (λ_{ex} = 472 nm, f = 0.1245) and close to the experimental values of **6**–**13** (λ_{ex} = 445–471 nm, cf. Table 1). The excited states involved can again be characterized as optically allowed π→π* transitions predominantly localized at the diaminoterephthalate moiety. The corresponding orbitals of **18** are displayed in Figure 4.

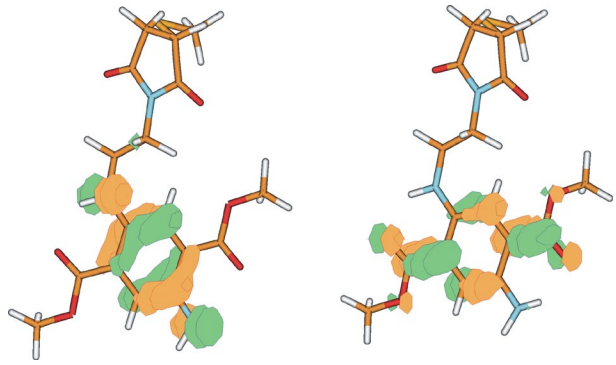

Figure 4. HOMO (left) and LUMO (right) of **18**. The lowest excited state corresponds to an optically allowed π→π* transition from the HOMO to the LUMO.

For **18**, this π→π* transition is involved in the corresponding fluorescence, which is predicted at a wavelength of λ_{em} = 558 nm with an oscillator strength of f = 0.1163 in excellent agreement with the experimental values (λ_{em} = 559–569 nm, cf. Table 1).

Similar to **18**, the simplified NiWa Orange model **17** exhibits an optically allowed $\pi \rightarrow \pi^*$ transition from the HOMO to the LUMO+1 as the second electronically excited state of the system. However, the first electronically excited, dark state responsible for a radiationless decay in NiWa Orange and **17** can be characterized as a HOMO to LUMO transition to a charge-transfer state, in which an electron is promoted from the diaminoterephthalate moiety to the maleimide unit. The corresponding orbitals are displayed in Figure 5.

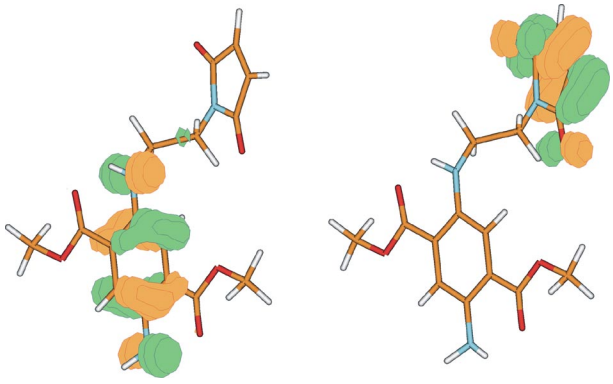

Figure 5. HOMO (left) and LUMO (right) of **17**. The lowest excited state corresponds to an optically forbidden charge-transfer transition from the HOMO to the LUMO.

As illustrated in Figure 5, the energetically low-lying charge-transfer excitation of **17** is not accessible by optical excitation due to a negligible HOMO–LUMO Franck–Condon orbital overlap, which results in a very small oscillator strength (λ_{ex} = 807 nm, f = 0.0001). However, this state plays the crucial role in quenching the fluorescence of **17** by nonadiabatic relaxation through a conical intersection.

Therefore, the general mechanistic picture of the fluorescence behavior is the same for NiWa Blue and NiWa Orange.

Monitoring the Ca^{2+} Switch of Recoverin with NiWa Orange II

Site-directed labeling of proteins at selected sites is a valuable approach in structure–function studies of proteins. Based on our previous experience with the neuronal Ca^{2+} sensor recoverin as a benchmark model for studying conformational changes by fluorescent probes,[10,12b] we investigated whether the dye NiWa Orange II **8** is suitable for detecting Ca^{2+}-induced conformational changes in recoverin, in particular, whether differences between the myristoylated and nonmyristoylated recoverin forms can be detected by this approach. Labeling of recoverin was performed successfully and yielded a 1:1 stoichiometry, which indicates free accessibility of the cysteine in the 39-position. No principle difference was observed, if we used a borate or carbonate buffer for the labeling procedure. Once conjugated to recoverin, NiWa Orange II exhibited a large increase in fluorescence emission at 580 nm, which was not sensitive to changes in free Ca^{2+} concentration (Figure 6, A). However, the spectrum also showed a shoulder at ca. 500 nm, the intensity of which increased with higher free Ca^{2+} concentration (compare spectra obtained at 58 nM and 500 μM free Ca^{2+} in Figure 6). Guided by our previous studies with NiWa-Blue-labeled recoverin,[10] we also observed that excitation of intrinsic Trp residues at 280 nm and emission between 320–360 nm triggered a FRET process and excited the covalently attached NiWa Orange II dye (Figure 6, B). Surprisingly, the large fluorescence emission peak at 580 nm disappeared and the shoulder at ca. 500 nm was blueshifted to 475 nm. Apparently, the fluorescence emission at 580 nm was completely quenched when endogenous Trp residues in recoverin were excited. Thus, the FRET recordings showed two maxima at 330 nm and at 475 nm. The signals were also Ca^{2+} dependent, exhibiting an increase at 330 nm and a decrease in intensity at 475 nm when the free Ca^{2+} concentration was lowered (Figure 6, B). The emission intensity changed with incremental changes of free Ca^{2+} concentra-

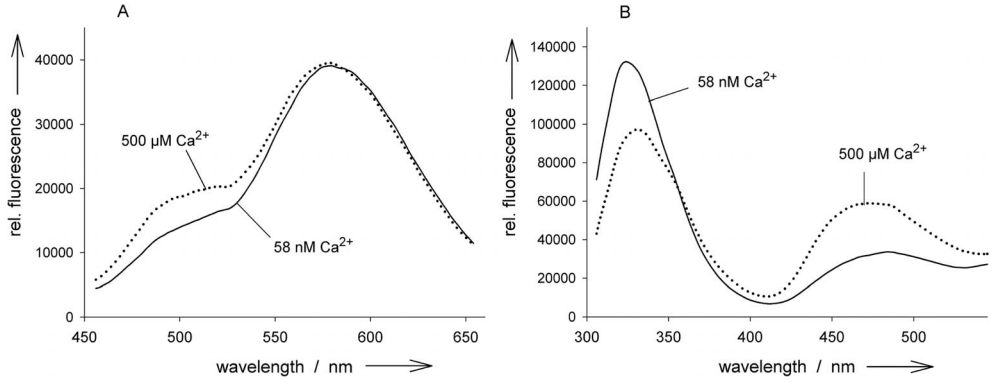

Figure 6. Emission spectra of myristoylated recoverin [2 μM in 80 mM buffer 4-(2-hydroxyethyl)-1-piperazineethanesulfonic acid (HEPES)-KOH, pH 7.5, 40 mM KCl, 1 mM dithiothreitol (DTT)] labeled with NiWa Orange II. Part A (left): emission scan in the presence of high Ca^{2+} concentration (500 μM, dotted line) and low Ca^{2+} concentration (58 nM, solid line); excitation of NiWa Orange II at λ_{ex} = 440 nm. Part B (right): FRET study of 2 μM NiWa-Orange-labeled recoverin. Intrinsic FRET was measured by excitation of Trp at 280 nm and the emission spectra were recorded between 300 and 550 nm. Buffer composition and Ca^{2+} concentration was as in Figure 6 A.

tion between 0.37 μM and 1000 μM, indicating a Ca^{2+}-dependent movement of one or more Trp residues in the vicinity of the thiol-attached dye. Superimposed FRET spectra recorded at different Ca^{2+} concentrations are shown in Figure 7 for myristoylated recoverin. Plotting the ratio of fluorescence emission at 475 nm and 330 nm (F_{475}/F_{330}) as a function of the Ca^{2+} concentration gave a dose response curve with an apparent K_D value of 18.4 μM (Figure 8, A). The same set of fluorescence recordings were performed with labeled nonmyristoylated recoverin and gave a similar general picture with respect to emission maxima and Ca^{2+} dependency (not shown). Analyzing the data by the same plot of F_{475}/F_{330} vs. Ca^{2+} yielded the curve shown in part B of Figure 8. The change in emission ratio was half maximal at 0.3 μM Ca^{2+}. These data are in perfect agreement with previous estimates of the dissociation constants of Ca^{2+} binding to recoverin.[18–20] Direct Ca^{2+}-binding studies on nonmyristoylated wildtype and mutant recoverin forms with disabled EF-hand Ca^{2+} binding sites showed that EF-hand 3 binds Ca^{2+} with a K_D of 0.1–0.26 μM and EF-hand 2 exhibits a lower affinity with a K_D of 6–7 μM.[19,20] The myristoyl group in recoverin serves as an allosteric modulator and lowers the affinity for Ca^{2+} resulting in an apparent K_D of 17–18 μM for the whole binding process.[18,19] Our fluorescence data on myristoylated recoverin matched exactly the affinity that was previously determined by direct binding studies with $^{45}Ca^{2+}$. Interestingly, for nonmyristoylated recoverin we determined by FRET analysis that the conformational change is half maximal at 0.3 μM Ca^{2+} and equal to the apparent K_D of the high affinity Ca^{2+} binding site in EF-hand 3. Previous NMR and X-ray crystallographic studies on wildtype and mutant recoverin forms indicate that binding of Ca^{2+} to the high affinity site in EF-hand 3 triggers a major conformational change, which includes a swiveling of the two domains in recoverin by 45°.[20,21] We conclude from our data that the distance between the FRET pair of Trp and the dye at the 39-position changes significantly during this domain rearrangement.

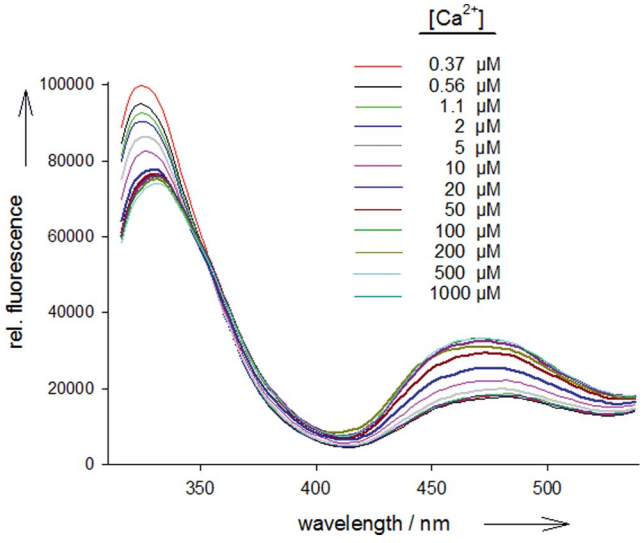

Figure 7. FRET emission scan of myristoylated recoverin labeled with NiWa Orange II. The spectra were recorded with 2 μM labeled recoverin at different Ca^{2+} concentrations as indicated in the inset. The excitation of intrinsic Trp was at 280 nm.

Conclusions

We had recently introduced NiWa Blue dyes, the fluorescence of which is turned on by conjugated addition of thiols (λ_{em} = 400 nm, λ_{ex} = 338 nm). We now have prepared NiWa Orange dyes with redshifted emission (λ_{em} = 560 nm, λ_{ex} = 470 nm). The diaminoterephthalate chromophore was electronically decoupled from the thiol-reactive maleimide group by introduction of an ethylenediamine spacer. Whereas the parent compound NiWa Orange I (**7**) possesses two maleimide functions, derived NiWa Orange II (**8**) and III (**11**) have a single thiol-reactive group.

In order to shine light on the mechanism of turning on the fluorescence of NiWa Blue and Orange dyes by thiol addition, we have performed computational studies. The thiol addition products in both, the blue and orange series, turned out to be normal fluorescence dyes with HOMO–LUMO transitions located at the aromatic chromophores of these compounds. In contrast, the nonfluorescent malei-

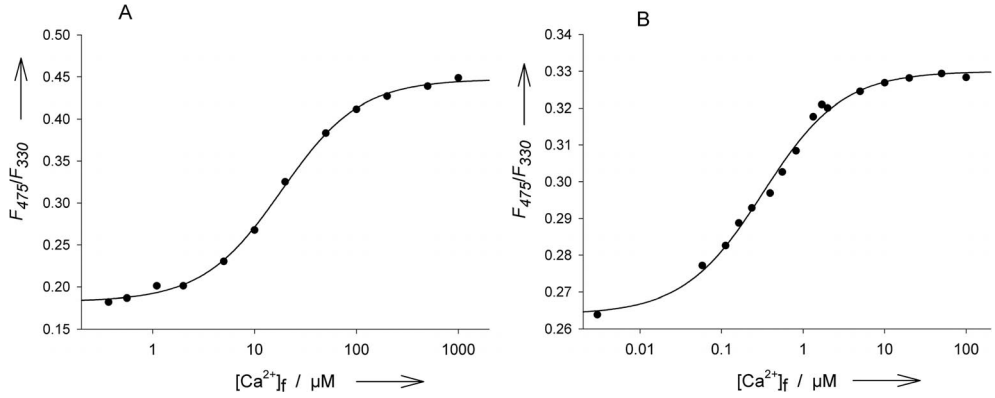

Figure 8. Ratio of fluorescence emission at 475 nm and 330 nm plotted as a function of the free Ca^{2+} concentration for myristoylated (A) and nonmyristoylated labeled recoverin (B). Sets of spectra as shown in Figure 7 were evaluated. The change was half maximal at 18 μM for myristoylated and at 0.3 μM for nonmyristoylated recoverin.

mides possess a different, lower LUMO located at the imide moiety of the molecule, but the excitation from the aromatic HOMO to the LUMO is optically forbidden because of a vanishing orbital overlap. Therefore, excitation of the electron occurs from the aromatic HOMO to the LUMO+1, which is also located at the six-membered ring. Interestingly, due to nonadiabatic coupling of the potential surfaces of the two excited states, the system will undergo a radiationless transition from LUMO+1 to LUMO, from which a further electronic relaxation to the HOMO is again optically forbidden. This mechanism is even applicable to the NiWa Orange systems, where the diaminoterephthalate and the maleimide parts of the molecule are quite distal. This scenario is significantly different from the fluorescence quenching mechanism postulated for the BODIPY derivative **2** (cf. Figure 1), where a strongly distance-dependent donor-excited photoinduced electron transfer was assumed.[5]

Recoverin is a neuronal calcium sensor protein, which plays a major role in the photoreceptor function in vertebrate retina. The protein adopts two significantly different conformations in the absence and presence of Ca^{2+}. Moreover, it has a single Cys residue at the 39-position, which covalently binds to NiWa Orange II **8**. A fluorescence emission is turned on by this conjugate addition. Excitation of a Trp residue in proximity to Cys-39 leads to FRET to NiWa Orange. The intensity of this FRET process is distance dependent and therefore sensitive to conformational changes of the protein induced by Ca^{2+}. An internal FRET study using excitation of Trp allowed us to monitor the critical Ca^{2+}-binding step that triggered the major conformational change in recoverin. Moreover, the Ca^{2+}-binding properties of myristoylated and nonmyristoylated recoverin could be clearly distinguished. The nonmyristoylated recoverin showed an apparent K_D of 0.3 μM Ca^{2+}. The myristoyl group in recoverin serves as an allosteric modulator and lowers the affinity for Ca^{2+}, therefore, the FRET study resulted in an apparent K_D of 18.4 μM Ca^{2+} in this case.

Experimental Section

General: Preparative column chromatography was carried out using Merck SiO_2 (0.035–0.070 mm, type 60 A) with hexane, CH_2Cl_2, and ethyl acetate (EtOAc) as eluents (for mixtures volume fractions are given). TLC was performed with Merck SiO_2 F_{254} plates on aluminum sheets. ^1H and ^{13}C NMR spectra were recorded with a Bruker Avance DRX 500. The multiplicities of carbon signals were determined with DEPT experiments. MS and HRMS spectra were obtained with a Finnigan MAT 95 (EI and CI) and a Waters Q-TOF Premier (ESI) spectrometer. IR spectra were recorded with a Bruker Tensor 27 spectrometer equipped with a GoldenGate diamond attenuated total reflectance (ATR) unit. Elemental analyses were measured with a Euro EA-CHNS instrument from HEKAtech. UV/Vis spectra were recorded with Perkin–Elmer LS 50 and Analytik Jena SPECORD 205 spectrometers. Fluorescence spectra were recorded with a Shimadzu RF-5301PC and a fluorescence spectrometer from Photon Technology International (Lamp Power supply Model LPS-220B and 810/814 Photomultiplier Detection System). Compound **5**[14] and *N*-Boc-1,2-diaminoethane[15] were prepared according to literature procedures. All other starting materials were commercially available.

Dimethyl 2,5-Bis[(2-*tert*-butoxycarbonylamino)ethylamino]terephthalate (6): A suspension of succinyl succinate **5** (367 mg, 1.61 mmol), *N*-Boc-ethylendiamine (1.03 g, 6.43 mmol) and glacial acetic acid (0.8 mL) in toluene (8 mL) was heated to reflux in a Dean–Stark apparatus for 16 h. The solution was diluted with EtOAc (75 mL) and washed with saturated aqueous $NaHCO_3$ solution (75 mL). The aqueous layer was extracted with EtOAc (75 mL), and the combined organic layers were dried ($MgSO_4$). After filtration and evaporation, the residue was chromatographed (SiO_2, hexane/EtOAc 2:1 with 2 vol.-% NEt_3). Fractions with R_f = 0.25 and 0.13 were collected, and the solvents were evaporated. The materials (662 mg) were redissolved in abs. DMF (10 mL), a solution of HCl in *i*PrOH (0.5 mL, 5–6 mol L^{-1}) was added, and under exclusion of moisture, synthetic air was passed through the solution for 5 h while heating the mixture to 50 °C. After cooling to ambient temperature, EtOAc (50 mL) and saturated aqueous $NaHCO_3$ solution (50 mL) were added to the mixture, and the aqueous layer was extracted with EtOAc (50 mL). The combined organic layers were dried ($MgSO_4$). After filtration and evaporation, the residue was chromatographed [SiO_2, gradient elution hexane/EtOAc 3:1 → 2:1 with 2 vol.-% NEt_3, R_f (hexane/EtOAc 2:1) = 0.25] to yield compound **6** (581 mg, 1.14 mmol, 71%) as a red solid, m.p. 154 °C. UV/Vis (CH_2Cl_2): λ_{max} (ε, $mol^{-1}\,dm^3\,cm^{-1}$) = 469 nm (5600); fluorescence (CH_2Cl_2): λ_{ex} = 469 nm; λ_{em} = 569 nm. ^1H NMR (500 MHz, $CDCl_3$): δ = 1.43 (s, 18 H), 3.32 (t, J = 5.6 Hz, 4 H), 3.38–3.42 (m, 4 H), 3.89 (s, 6 H), 4.80 (br. s, 2 H), 6.90 (br. s, 2 H), 7.33 (s, 2 H) ppm. $^{13}C\{^1H\}$ NMR (125 MHz, $CDCl_3$): δ = 28.32 (6 CH_3), 39.88 (2 CH_2), 43.61 (2 CH_2), 51.85 (2 CH_3), 79.28 (2 C), 114.15 (2 CH), 116.91 (2 C), 140.99 (2 C), 155.96 (2 C), 168.16 (2 C) ppm. IR (ATR): $\tilde{\nu}$ = 3362 (s), 2968 (m), 2948 (m), 1687 (vs), 1522 (vs), 1467 (m), 1439 (m), 1420 (m), 1392 (w), 1366 (w), 1332 (w), 1291 (m), 1272 (m), 1207 (vs), 1160 (vs), 1119 (vs), 1092 (s), 1037 (m), 998 (m), 969 (m), 907 (w), 872 (m), 849 (w), 788 (s), 759 (w) cm^{-1}. HRMS (ESI, pos. mode): calcd. for $C_{24}H_{39}N_4O_8$ $[M + H]^+$ 511.2768; found 511.2779. $C_{24}H_{38}N_4O_8$ (510.58): calcd. C 56.46, H 7.50, N 10.97; found C 56.18, H 7.81, N 11.17.

Dimethyl 2,5-Bis[2-(2,5-dioxo-2,5-dihydropyrrol-1-yl)ethylamino]-terephthalate (NiWa Orange I) (7): A solution of biscarbamate **6** (894 mg, 1.75 mmol) in TFA (5 mL) was stirred at 23 °C for 30 min. Glacial acetic acid (6.4 mL) and maleic anhydride (687 mg, 7.01 mmol) were added, and the mixture was further heated at 95 °C for 3 d. The solution was then diluted with EtOAc (75 mL) and saturated $NaHCO_3$ solution (75 mL), and the layers were separated. The aqueous layer was extracted with EtOAc (2 × 75 mL), and the combined organic layers were dried ($MgSO_4$). After filtration and evaporation, the residue was chromatographed (SiO_2, hexane/EtOAc 2:1 → 1:1 → 1:2 → EtOAc). The first fraction [R_f (hexane/EtOAc 1:2) = 0.43] contained the title compound **7** (262 mg, 0.557 mmol, 32%) as an orange solid; m.p. 223 °C. No byproduct **8** was isolated in this case. UV/Vis (CH_2Cl_2): λ_{max} (ε, $mol^{-1}\,dm^3\,cm^{-1}$) = 462 nm (290). ^1H NMR (500 MHz, $CDCl_3$): δ = 3.40–3.65 (m, 4 H), 3.80 (t, J = 6.2 Hz, 4 H), 3.90 (s, 6 H), 6.69 (s, 4 H), 6.89 (br. s, 2 H), 7.34 (s, 2 H) ppm. $^{13}C\{^1H\}$ NMR (125 MHz, $CDCl_3$): δ = 37.11 (2 CH_2), 41.94 (2 CH_2), 51.96 (2 CH_3), 114.20 (2 CH), 117.26 (2 C), 134.15 (4 CH), 140.67 (2 C), 168.08 (2 C), 170.62 (4 C) ppm. IR (ATR): $\tilde{\nu}$ = 3354 (m), 3118 (w), 2953 (w), 2922 (m), 2849 (m), 1690 (vs), 1592 (w), 1533 (m), 1467 (w), 1439 (m), 1406 (m), 1360 (m), 1333 (m), 1258 (m), 1209 (vs), 1158 (m), 1110 (vs), 1089 (m), 1057 (m), 998 (m), 962 (m), 912 (m), 874 (w),

853 (w), 834 (vs), 787 (s), 721 (w), 696 (vs) cm^{-1}. HRMS (EI, 70 eV): calcd. for $C_{22}H_{22}N_4O_8$ $[M]^+$ 470.1438; found 470.1429.

Dimethyl 2-[2-(3-Acetoxy-2,5-dioxopyrrolidin-1-yl)ethylamino]-5-[2-(2,5-dioxo-2,5-dihydropyrrol-1-yl)ethylamino]terephthalate (NiWa Orange II) (8): A solution of biscarbamate **6** (410 mg, 0.803 mmol) in CH_2Cl_2 (4 mL) and TFA (2 mL) was stirred at 23 °C for 1 h. Glacial acetic acid (3 mL) and maleic anhydride (315 mg, 3.21 mmol) were added, and the resulting mixture was further heated at 90 °C for 2 d. The solution was then diluted with EtOAc (90 mL) and H_2O (40 mL), and the layers were separated. The organic layer was extracted with H_2O (40 mL) and dried ($MgSO_4$). After filtration and evaporation, the residue was chromatographed (SiO_2, hexane/EtOAc 2:1 → 1:1 → 1:2). The first fraction [R_f (hexane/EtOAc 1:2) = 0.43] contained compound **7** (56 mg, 0.12 mmol, 15%) as an orange solid. From the second fraction [R_f (hexane/EtOAc 1:2) = 0.33], compound **8** (40 mg, 75 μmol, 9%) was isolated as a byproduct; m.p. 128 °C. UV/Vis (CH_2Cl_2): λ_{max} (ε, $mol^{-1}\,dm^3\,cm^{-1}$) = 446 nm (6700). ^1H NMR (500 MHz, $CDCl_3$): δ = 2.14 (s, 3 H), 2.64 (dd, J = 4.8, J = 18.2 Hz, 1 H), 3.15 (dd, J = 8.7, J = 18.3 Hz, 1 H), 3.40–3.51 (m, 4 H), 3.78–3.82 (m, 2 H), 3.82–3.86 (m, 2 H), 3.90 (s, 3 H), 3.91 (s, 3 H), 5.43 (dd, J = 4.8, J = 8.6 Hz, 1 H), 6.70 (s, 2 H), 7.39 (s, 1 H), 7.40 (s, 1 H) ppm; the two NH protons are not detectable. $^{13}C\{^1H\}$ NMR (125 MHz, $CDCl_3$, 330 K): δ = 20.38 (CH_3), 35.72 (CH_2), 37.23 (CH_2), 38.47 (CH_2), 41.11 (CH_2), 42.02 (CH_2), 51.91 (2 CH_3), 67.50 (CH), 114.46 (CH), 114.60 (CH), 117.46 (C), 117.74 (C), 134.16 (2 CH), 140.50 (C), 140.93 (C), 168.02 (C), 168.11 (C), 169.64 (C), 170.54 (2 C), 173.05 (C), 173.31 (C) ppm. IR (ATR): $\tilde{\nu}$ = 3355 (w), 3111 (w), 2953 (w), 2848 (w), 1693 (vs), 1601 (w), 1533 (m), 1438 (m), 1405 (m), 1358 (m), 1335 (m), 1213 (vs), 1110 (s), 1040 (m), 997 (w), 964 (w), 913 (m), 873 (w), 830 (m), 788 (m), 728 (m), 696 (s), 648 (w) cm^{-1}. HRMS (EI, 70 eV): calcd. for $C_{24}H_{26}N_4O_{10}$ $[M]^+$ 530.1649; found 530.1641.

Turn On of NiWa Orange II (8) with Glutathione (*G*SH), Formation of 9: DMSO (1 mL) was added to a mixture of acetoxy adduct **8** (1.3 mg, 2.5 μmol) and *G*SH (10 mg, 33 μmol), and the resulting mixture was stirred for 20 min at 23 °C. It was then diluted with DMSO (9 mL) and further analyzed. UV/Vis (DMSO): λ_{max} (ε, $mol^{-1}\,dm^3\,cm^{-1}$) = 469 nm (6700); fluorescence (DMSO): λ_{ex} = 469 nm; λ_{em} = 568 nm. HRMS (ESI, pos. mode): calcd. for $C_{34}H_{44}N_7O_{16}S$ $[M + H]^+$ 838.2565; found 838.2551.

Dimethyl 2,5-Bis{2-[3-(benzylsulfanyl)-2,5-dioxopyrrolidin-1-yl]ethylamino}terephthalate (10): A solution of bismaleinimide **7** (25 mg, 53 μmol), BnSH (32 mg, 0.26 mmol) and NEt_3 (19 mg, 0.19 mmol) in CH_2Cl_2 (2 mL) was stirred at 23 °C for 1 d. The solvent was removed under reduced pressure, and the residue was chromatographed [SiO_2, gradient elution hexane/EtOAc 2:1 → 1:1 → EtOAc, R_f (hexane/EtOAc 2:1) = 0.09] to yield the compound **10** (33 mg, 46 μmol, 87%) as a red solid, m.p. 70 °C. UV/Vis (CH_2Cl_2): λ_{max} (ε, $mol^{-1}\,dm^3\,cm^{-1}$) = 467 nm (3400); fluorescence (CH_2Cl_2): λ_{ex} = 467 nm; λ_{em} = 559 nm. ^1H NMR (500 MHz, $CDCl_3$, 330 K): δ = 2.43 (dd, J = 3.9, J = 18.6 Hz, 2 H), 2.96 (dd, J = 9.2, J = 18.6 Hz, 2 H), 3.47 (t, J = 6.1 Hz, 4 H), 3.54 (dd, J = 3.9, J = 9.2 Hz, 2 H), 3.77–3.84 (m, 4 H), 3.88 (d, J = 13.4 Hz, 2 H), 3.91 (s, 6 H), 4.19 (d, J = 13.5 Hz, 2 H), 6.87 (br. s, 2 H), 7.27–7.30 (m, 2 H), 7.31–7.36 (m, 4 H), 7.37–7.41 (m, 6 H) ppm. $^{13}C\{^1H\}$ NMR (125 MHz, $CDCl_3$, 330 K): δ = 35.66 (2 CH_2), 36.00 (2 CH_2), 37.95 (2 CH), 38.41 (2 CH_2), 41.13 (2 CH_2), 51.87 (2 CH_3), 114.43 (2 CH), 117.56 (2 C), 127.53 (2 CH), 128.69 (4 CH), 129.16 (4 CH), 136.94 (2 C), 140.79 (2 C), 168.07 (2 C), 174.48 (2 C), 176.52 (2 C) ppm. IR (ATR): $\tilde{\nu}$ = 3373 (m), 3060 (w), 3030 (w), 2951 (m), 2859 (w), 1177 (w), 1698 (vs), 1604 (w), 1578 (w), 1532 (s), 1497 (w), 1456 (m), 1437 (m), 1420 (m), 1397 (s), 1359 (m), 1336 (m), 1216 (vs), 1175 (s), 1116 (s), 1074 (m), 1031 (w), 991 (w), 920 (w), 874 (w) cm^{-1}. HRMS (EI, 70 eV): calcd. for $C_{36}H_{38}N_4O_8S_2$ $[M]^+$ 718.2131; found 718.2148.

Conversion of Bisimide 7 with Hexadecanethiol: A solution of 1-hexadecanethiol (0.12 mmol, 8.1 mL, 0.015 mol L^{-1} in CH_2Cl_2) was added (cooling with an ice-water bath) to a solution of bismaleinimide **7** (114 mg, 0.242 mmol) and NEt_3 (100 mg, 0.988 mmol) in CH_2Cl_2 (4 mL). The mixture was warmed to 23 °C and then stirred for 24 h. The solvent was evaporated under reduced pressure, and the crude solid was purified by chromatography (SiO_2, gradient elution with hexane/CH_2Cl_2/EtOAc 2:1:1 → 1:1:1 → CH_2Cl_2/EtOAc 1:1) to yield bis adduct **12** (18 mg, 18 μmol, 8%) in the first fraction [R_f(SiO_2, CH_2Cl_2/EtOAc 1:1) = 0.53]. The second fraction [R_f (SiO_2, CH_2Cl_2/EtOAc 1:1) = 0.30] was mono adduct **11** (20 mg, 27 μmol, 11%; NiWa Orange III). Finally, starting material **7** (22 mg, 47 μmol, 19%) was obtained as the third fraction [R_f (SiO_2, CH_2Cl_2/EtOAc 1:1) = 0.11].

Dimethyl 2-[2-(2,5-Dioxo-2,5-dihydropyrrol-1-yl)ethylamino]-5-[2-(3-hexadecylsulfanyl-2,5-dioxopyrrolidin-1-yl)ethylamino]terephthalate (NiWa Orange III) (11): M.p. 186 °C. UV/Vis (CH_2Cl_2): λ_{max} (ε, $mol^{-1}\,dm^3\,cm^{-1}$) = 468 nm (2500). ^1H NMR (500 MHz, $CDCl_3$): δ = 0.88 (t, J = 6.9 Hz, 3 H), 1.22–1.30 (m, 23 H), 1.32–1.39 (m, 2 H), 1.54–1.66 (m, 3 H), 2.52 (dd, J = 3.6, J = 18.6 Hz, 1 H), 2.71 (ddd, J = 6.8, J = 8.3, J = 15.0 Hz, 1 H), 2.85 (ddd, J = 6.3, J = 8.7, J = 14.4 Hz, 1 H), 3.14 (dd, J = 8.0, J = 18.8 Hz, 1 H), 3.43 (q, J = 6.5 Hz, 4 H), 3.72 (dd, J = 3.6, J = 8.1 Hz, 1 H), 3.79–3.83 (m, 4 H), 3.90 (s, 3 H), 3.91 (s, 3 H), 6.70 (s, 2 H), 7.37 (s, 1 H), 7.42 (s, 1 H) ppm; the two NH protons are not detectable. $^{13}C\{^1H\}$ NMR (125 MHz, $CDCl_3$): δ = 14.05 (CH_3), 22.67 (CH_2), 28.83 (CH_2), 29.10 (CH_2), 29.20 (CH_2), 29.35 (CH_2), 29.50 (CH_2), 29.59 (2 CH_2), 29.66 (2 CH_2), 29.69 (4 CH_2), 31.77 (CH_2), 31.93 (CH_2), 36.27 (CH_2), 37.11 (CH_2), 38.23 (CH_2), 39.33 (CH), 42.11 (CH_2), 51.98 (CH_3), 52.03 (CH_3), 114.52 (2 CH), 117.39 (2 C), 134.18 (2 CH), 141.05 (2 C), 168.00 (2 C), 170.56 (2 C), 174.76 (C), 176.59 (C) ppm. IR (ATR): $\tilde{\nu}$ = 3357 (w), 2919 (m), 2850 (m), 1692 (vs), 1537 (m), 1439 (m), 1404 (m), 1360 (m), 1336 (m), 1220 (vs), 1112 (vs), 963 (w), 911 (w), 874 (w), 838 (m), 788 (s), 721 (w), 697 (s) cm^{-1}. HRMS (EI, 70 eV): calcd. for $C_{38}H_{56}N_4O_8S$ $[M]^+$ 728.3819; found 728.3806.

Dimethyl 2,5-Bis{2-[3-(hexadecylsulfanyl)-2,5-dioxopyrrolidin-1-yl]-ethylamino}terephthalate (12): M.p. 165 °C. UV/Vis (CH_2Cl_2): λ_{max} (ε, $mol^{-1}\,dm^3\,cm^{-1}$) = 467 nm (4200); fluorescence (CH_2Cl_2): λ_{ex} = 467 nm; λ_{em} = 561 nm. ^1H NMR (500 MHz, $CDCl_3$, 328 K): δ = 0.89 (t, J = 6.8 Hz, 6 H), 1.24–1.33 (m, 48 H), 1.33–1.45 (m, 4 H), 1.56–1.69 (m, 4 H), 2.51 (dd, J = 3.6, J = 18.5 Hz, 2 H), 2.70–2.76 (m, 2 H), 2.85 (ddd, J = 6.3, J = 8.1, J = 18.7 Hz, 2 H), 3.09 (dd, J = 9.1, J = 18.5 Hz, 2 H), 3.45 (t, J = 6.3 Hz, 4 H), 3.68 (dd, J = 3.7, J = 9.0 Hz, 2 H), 3.77–3.82 (m, 4 H), 3.91 (s, 6 H), 7.37 (s, 2 H) ppm; the two NH protons are not detectable. $^{13}C\{^1H\}$ NMR (125 MHz, $CDCl_3$, 328 K): δ = 14.00 (2 CH_3), 22.67 (2 CH_2), 28.83 (2 CH_2), 29.15 (2 CH_2), 29.20 (2 CH_2), 29.34 (2 CH_2), 29.50 (2 CH_2), 29.59 (2 CH_2), 29.69 (4 CH_2), 29.69 (6 CH_2), 31.80 (2 CH_2), 31.93 (2 CH_2), 36.29 (2 CH_2), 38.39 (2 CH_2), 39.39 (2 CH), 42.22 (2 CH_2), 51.90 (2 CH_3), 114.53 (2 CH), 117.60 (2 C), 140.75 (2 C), 168.07 (2 C), 174.62 (2 C), 176.57 (2 C) ppm; signals for two CH_2 groups at approx. 37 ppm are not detectable. IR (ATR): $\tilde{\nu}$ = 3372 (w), 2917 (s), 2850 (m), 1769 (w), 1692 (vs), 1539 (m), 1467 (m), 1439 (m), 1401 (m), 1342 (m), 1220 (s), 1203 (s), 1116 (s), 949 (w), 873 (w), 788 (m), 720 (w), 694 (w) cm^{-1}. HRMS (EI, 70 eV): calcd. for $C_{54}H_{90}N_4O_8S_2$ $[M]^+$ 986.6200; found 986.6209.

Turn On of NiWa Orange III (11) with Glutathione (*G*SH), Formation of Product 13: DMSO (1 mL) was added to a mixture of thiol adduct **11** (0.9 mg, 1.3 μmol) and *G*SH (10 mg, 33 μmol) and the resulting mixture was stirred for 20 min at 23 °C. It was then diluted with DMSO (9 mL) and further analyzed. UV/Vis (DMSO): λ_{max} (ε, $mol^{-1}\,dm^3\,cm^{-1}$) = 469 nm (2100); fluorescence (DMSO): λ_{em} = 565 nm; λ_{ex} = 469 nm. HRMS (ESI, pos. mode): calcd. for $C_{48}H_{74}N_7O_{14}S_2$ $[M + H]^+$ 1036.4735; found 1036.4720.

Preparation and Labeling of Recoverin: Bovine recoverin was heterologously expressed in *E. coli* (BL21 strain) exactly as described previously.[10,12] In order to express myristoylated recoverin in *E. coli* cells these were cotransformed with the plasmid carrying the gene for yeast *N*-myristoyl-transferase (pBB131). Myristoylated recoverin was expressed, purified, and analyzed by HPLC as described before.[18] For labeling with NiWa Orange II, we dissolved 0.5 mg of lyophilized recoverin in 0.45 mL carbonate or borate coupling buffer (carbonate buffer: 20 mM $NaHCO_3$/NaOH pH 10.0, 100 mM NaCl; borate buffer: 20 mM H_3BO_3/NaOH pH 10.0, 100 mM NaCl). The dye NiWa Orange II (**8**) (50 μL of a 1.9 mM solution in DMSO) was added to the recoverin solution and the mixture was incubated under gentle shaking for 1.5 h at room temperature in the dark. Unreacted dye was removed by passing the solution over a short gel filtration column (PD10 containing Sephadex G25 material with a void volume of 2.5 mL, GE Healthcare). The PD10 column was equilibrated in fluorescence buffer (80 mM HEPES-KOH pH 7.5, 40 mM KCl, 1 mM DTT) when labeled recoverin was further used for fluorescence studies. For this purpose the recoverin solution after passing over the PD 10 column was diluted with 10 mL of fluorescence buffer to yield a final volume of 13.5 mL. The stoichiometry of bound dye was determined by measuring the extinction of the bound dye at 440 nm using a UV/Vis spectrophotometer (SPECORD 205, Analytik Jena). The protein concentration was determined with the Coomassie blue dye method of Bradford[22] yielding a stoichiometry of approx. 1:1 for nonmyristoylated and myristoylated recoverin.

Fluorescence Recordings: For each recording 0.96 mL of labeled recoverin stock was mixed with 0.04 mL of Ca^{2+}-EGTA buffer (2 mM) or $CaCl_2$ to yield final free Ca^{2+} concentrations from 0.37 μM to 1 mM. Those concentrations of free Ca^{2+} were adjusted by mixtures of K_2H_2EGTA (EGTA = ethylene glycol bis(2-aminoethyl ether) tetraacetic acid, 50 mM) and CaH_2EGTA (50 mM) as described previously.[23] Concentrations of free Ca^{2+} above 2 μM were adjusted by adding $CaCl_2$ at the desired final concentration. The fluorescence emission spectra of 2 μM labeled recoverin were measured with a fluorescence spectrometer from Photon Technology International (Lamp Power supply Model LPS-220B and 810/814 Photomulitplier Detection System). The sample was excited at 440 nm and the emission spectra were recorded from 450–650 nm. FRET from endogenous Trp residues to the conjugated dye was measured by setting the excitation wavelength to 280 nm and recording the emission spectra from 300 to 550 nm. Recording and data analysis was performed with the photon Technology International software package FELIX32.

Supporting Information (see footnote on the first page of this article): Additional fluorescence spectra and ^1H and ^{13}C NMR spectra of all reported compounds.

Acknowledgments

We gratefully acknowledge support from the Deutsche Forschungsgemeinschaft (DFG).

[1] For reviews, see: a) A. Mayer, S. Neuenhofer, *Angew. Chem.* **1994**, *106*, 1097–1126; *Angew. Chem. Int. Ed. Engl.* **1994**, *33*, 1044–1072; b) X. Chen, Y. Zhou, X. Peng, J. Yoon, *Chem. Soc. Rev.* **2010**, *39*, 2120–2135; c) T. Nagano, *Proc. Jpn. Acad., Ser. B* **2010**, *86*, 837–847.

[2] a) K. K.-W. Lo, W.-K. Hui, D. C.-M. Ng, K.-K. Cheung, *Inorg. Chem.* **2002**, *41*, 40–46; b) P. Ge, P. R. Selvin, *Bioconjugate Chem.* **2003**, *14*, 870–876; c) S. Girouard, M.-H. Houle, A. Grandbois, J. W. Keillor, S. W. Michnick, *J. Am. Chem. Soc.* **2005**, *127*, 559–566; d) J. Weh, A. Duerkop, O. S. Wolfbeis, *ChemBioChem* **2007**, *8*, 122–128; e) G.-L. Li, K.-Y. Kung, L. Zou, H.-C. Chong, Y.-C. Leung, K.-H. Wong, M.-K. Wong, *Chem. Commun.* **2012**, *48*, 3527–3529.

[3] P. Y. Reddy, S. Kondo, S. Fujita, T. Toru, *Synthesis* **1998**, 999–1002.

[4] a) L. Yi, H. Li, L. Sun, L. Liu, C. Zhang, Z. Xi, *Angew. Chem.* **2009**, *121*, 4094–4097; *Angew. Chem. Int. Ed.* **2009**, *48*, 4034–4037; b) X. Zhang, X. Ren, Q.-H. Xu, K. P. Loh, Z.-K. Chen, *Org. Lett.* **2009**, *11*, 1257–1260; c) L. Peng, G. Zhang, D. Zhang, J. Xiang, R. Zhao, Y. Wang, D. Zhu, *Org. Lett.* **2009**, *11*, 4014–4017; d) H. S. Jung, K. C. Ko, G.-H. Kim, A.-R. Lee, Y.-C. Na, C. Kang, J. Y. Lee, J. S. Kim, *Org. Lett.* **2011**, *13*, 1498–1501; e) S.-Y. Lim, S. Lee, S. B. Park, H.-J. Kim, *Tetrahedron Lett.* **2011**, *52*, 3902–3904; f) X.-D. Jiang, J. Zhang, X. Shao, W. Zhao, *Org. Biomol. Chem.* **2012**, *10*, 1966–1968.

[5] T. Matsumoto, Y. Urano, T. Shoda, H. Kojima, T. Nagano, *Org. Lett.* **2007**, *9*, 3375–3377.

[6] a) H. Liebermann, *Justus Liebigs Ann. Chem.* **1914**, *404*, 272–321; b) For a review, see: S. S. Labana, L. L. Labana, *Chem. Rev.* **1967**, *67*, 1–18.

[7] Y. Zhang, J. Christoffers, *Synthesis* **2007**, 3061–3067.

[8] a) S. D. Ohmura, T. Moriuchi, T. Hirao, *Tetrahedron Lett.* **2010**, *51*, 3190–3192; b) M. Shimizu, Y. Asai, Y. Takeda, A. Yamatani, T. Hiyama, *Tetrahedron Lett.* **2011**, *52*, 4084–4089.

[9] a) Y. Zhang, P. Starynowicz, J. Christoffers, *Eur. J. Org. Chem.* **2008**, 3488–3495; b) R. Pflantz, J. Christoffers, *Chem. Eur. J.* **2009**, *15*, 2200–2209.

[10] N. Wache, C. Schröder, K.-W. Koch, J. Christoffers, *ChemBioChem* **2012**, *13*, 993–998.

[11] I. I. Senin, K.-W. Koch, M. Akhtar, P. P. Philippov, *Adv. Exp. Med. Biol.* **2003**, *514*, 69–99.

[12] a) O. H. Weiergräber, I. I. Senin, E. Y. Zernii, V. A. Churumova, N. A. Kovaleva, A. A. Nazipova, S. E. Permyakov, E. A. Permyakov, P. P. Philippov, J. Granzin, K.-W. Koch, *J. Biol. Chem.* **2006**, *281*, 37594–37602; b) T. Gensch, K. E. Komolov, I. I. Senin, P. P. Philippov, K.-W. Koch, *Proteins Struct. Funct. Bioinf.* **2007**, *66*, 492–499.

[13] H. Kollmann, S. F. Becker, J. Shirdel, A. Scholten, A. Ostendorp, C. Lienau, K.-W. Koch, *ACS Chem. Biol.* **2012**, *7*, 1006–1014.

[14] D. Seebach, T. Hoffmann, F. N. M. Kühnle, J. N. Kinkel, M. Schulte, *Helv. Chim. Acta* **1995**, *78*, 1525–1540.

[15] T. L. Foley, A. Yasgar, C. J. Garcia, A. Jadhav, A. Simeonov, M. D. Burkart, *Org. Biomol. Chem.* **2010**, *8*, 4601–4606.

[16] a) J. R. Lakowicz, *Principles of Fluorescence Spectroscopy*, 3rd ed. Springer, New York, **2006**, p. 54; b) For fluorescein as standard, see: G. Weber, F. W. J. Teale, *Trans. Faraday Soc.* **1957**, *53*, 646–655.

[17] M. J. Frisch, G. W. Trucks, H. B. Schlegel, G. E. Scuseria, M. A. Robb, J. R. Cheeseman, G. Scalmani, V. Barone, B. Mennucci, G. A. Petersson, H. Nakatsuji, M. Caricato, X. Li, H. P. Hratchian, A. F. Izmaylov, J. Bloino, G. Zheng, J. L. Sonnenberg, M. Hada, M. Ehara, K. Toyota, R. Fukuda, J. Hasegawa, M. Ishida, T. Nakajima, Y. Honda, O. Kitao, H. Nakai, T. Vreven, J. A. Montgomery Jr, J. E. Peralta, F. Ogliaro, M. Bearpark, J. J. Heyd, E. Brothers, K. N. Kudin, V. N. Staroverov, R. Kobayashi, J. Normand, K. Raghavachari, A. Rendell, J. C. Burant, S. S. Iyengar, J. Tomasi, M. Cossi, N. Rega, J. M. Millam, M. Klene, J. E. Knox, J. B. Cross, V. Bakken, C. Ad-

amo, J. Jaramillo, R. Gomperts, R. E. Stratmann, O. Yazyev, A. J. Austin, R. Cammi, C. Pomelli, J. W. Ochterski, R. L. Martin, K. Morokuma, V. G. Zakrzewski, G. A. Voth, P. Salvador, J. J. Dannenberg, S. Dapprich, A. D. Daniels, Ö. Farkas, J. B. Foresman, J. V. Ortiz, J. Cioslowski, D. J. Fox, *Gaussian 09*, revision A.1, Gaussian, Inc., Wallingford CT, **2009**.

[18] I. I. Senin, T. Fischer, K. E. Komolov, D. V. Zinchenko, P. P. Philippov, K.-W. Koch, *J. Biol. Chem.* **2002**, *277*, 50365–50372.

[19] J. B. Ames, T. Porumb, T. Tanaka, M. Ikura, L. Stryer, *J. Biol. Chem.* **1995**, *270*, 4526–4533.

[20] O. H. Weiergräber, I. I. Senin, P. P. Philippov, J. Granzin, K.-W. Koch, *J. Biol. Chem.* **2003**, *278*, 22972–22979.

[21] J. B. Ames, N. Hamasaki, T. Molchanova, *Biochemistry* **2002**, *41*, 5776–5787.

[22] M. M. Bradford, *Anal. Biochem.* **1976**, *72*, 248–254.

[23] P. Behnen, A. Scholten, N. Rätscho, K.-W. Koch, *J. Biol. Inorg. Chem.* **2009**, *14*, 89–99.

Received: July 3, 2012
Published Online: ■

Fluorescent Probes

A Click Turns It On: Maleimide-functionalized diaminoterephthalates (NiWa Orange) are thiol-reactive fluorescence probes. Whereas the dye itself shows no fluorescence, it is turned on by the conjugate addition of the thiol. NiWa Orange was used to label recoverin. Its Ca^{2+}-dependent conformational change was traced by Förster resonance energy transfer of a tryptophan residue to NiWa Orange.

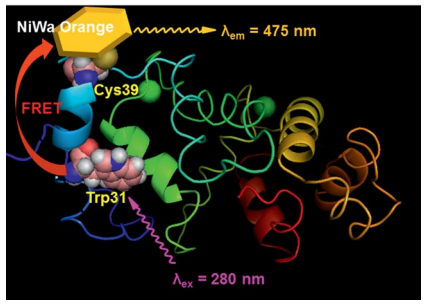

N. Wache, A. Scholten, T. Klüner, K.-W. Koch, J. Christoffers* 1–12

Turning On Fluorescence with Thiols – Synthetic and Computational Studies on Diaminoterephthalates and Monitoring the Switch of the Ca^{2+} Sensor Recoverin

Keywords: Fluorescent probes / Sensors / Calcium

